

## Research



**Cite this article:** Di Santo V. 2019 Ocean acidification and warming affect skeletal mineralization in a marine fish. *Proc. R. Soc. B* **286**: 20182187.  
<http://dx.doi.org/10.1098/rspb.2018.2187>

Received: 28 September 2018

Accepted: 11 December 2018

**Subject Category:**

Morphology and biomechanics

**Subject Areas:**

biomechanics, physiology

**Keywords:**

acidification, global warming, mineralization, elasmobranch, *Leucoraja erinacea*, micro-CT

**Author for correspondence:**

Valentina Di Santo

e-mail: [vdisanto@fas.harvard.edu](mailto:vdisanto@fas.harvard.edu)

Electronic supplementary material is available online at <https://doi.org/10.6084/m9.figshare.c.4339445>.

# Ocean acidification and warming affect skeletal mineralization in a marine fish

Valentina Di Santo

Museum of Comparative Zoology, Harvard University, 26 Oxford Street, Cambridge, MA, USA

VD, 0000-0002-5419-3747

Ocean acidification and warming are known to alter, and in many cases decrease, calcification rates of shell and reef building marine invertebrates. However, to date, there are no datasets on the combined effect of ocean pH and temperature on skeletal mineralization of marine vertebrates, such as fishes. Here, the embryos of an oviparous marine fish, the little skate (*Leucoraja erinacea*), were developmentally acclimatized to current and increased temperature and CO<sub>2</sub> conditions as expected by the year 2100 (15 and 20°C, approx. 400 and 1100 µatm, respectively), in a fully crossed experimental design. Using micro-computed tomography, hydroxyapatite density was estimated in the mineralized portion of the cartilage in jaws, crura, vertebrae, denticles and pectoral fins of juvenile skates. Mineralization increased as a consequence of high CO<sub>2</sub> in the cartilage of crura and jaws, while temperature decreased mineralization in the pectoral fins. Mineralization affects stiffness and strength of skeletal elements linearly, with implications for feeding and locomotion performance and efficiency. This study is, to my knowledge, the first to quantify a significant change in mineralization in the skeleton of a fish and shows that changes in temperature and pH of the oceans have complex effects on fish skeletal morphology.

## 1. Introduction

Anthropogenic activity has caused an increase in atmospheric concentrations of carbon dioxide (pCO<sub>2</sub>) that has now reached about 400 ppm (in 2018), a growth of approximately 41% since pre-Industrial Revolution levels, which produced a rise in the global average temperature of 0.8°C and a decrease of 0.1 unit pH [1]. Models of human activity continuing in 'business-as-usual' project an additional increase in global temperature of up to 5°C and a decline of an additional 0.4 units by the end of 2100, if emissions are not significantly curbed [2]. Therefore, aquatic organisms are expected to be challenged simultaneously by at least two climate-related stressors, warming and acidification. Not surprisingly, in the past years, a crucial quest for physiologists has been to identify responses of organisms to these major stressors in order to forecast outcomes of environmental change on ecosystems [3].

Marine ectotherms have an intimate relationship with their thermal environment, as virtually every physiological process is, at some degree, affected by ambient temperature [4,5]. In fact, in the past century, biologists have successfully and methodically characterized this relationship by quantifying thermal niches, limits and optimal conditions for physiological performance in a wide range of organisms [4,6]. Rates of physiological processes respond relatively rapidly to changes in temperature, and these have been quantified across different time scales. On the other hand, the effects of ocean acidification on fishes have been investigated to a much lesser degree. Most of the work on ocean acidification has focused on calcifying invertebrates, especially on the severe reduction in shell and exoskeleton formation when exposed to low pH conditions, making them important sentinels of environmental change [7–11].

Ocean acidification alters behaviour, escape response, development and activity in several species of fish [12–15]. Additionally, several studies have now documented an increase in calcification of the otolith (ear stone, made of calcium

carbonate) of different species of fish as a consequence of ocean acidification [16,17]. In a study that exposed larval cobia *Rachycentron canadum* to simulated conditions expected by year 2300 (approx. 2100  $\mu\text{atm}$ ), the otolith density, volume and area increased; however, no effect was found when larvae were exposed to lower  $\text{pCO}_2$  conditions (approx. 800  $\mu\text{atm}$ ) [16]. A similar result was found in the clownfish *Amphiprion percula*, which showed an increase in otolith size and shape at 1721  $\mu\text{atm}$   $\text{CO}_2$  but not at 1050  $\mu\text{atm}$   $\text{pCO}_2$  [18]. However, larvae of white sea bass *Atractoscion nobilis* exhibit larger otoliths when compared with a control [17]. Although otoliths are crucial for fishes to detect pressure, auditory stimuli and to maintain postural equilibrium [15,16], no study to date has evaluated the effects of ocean acidification and warming on fish skeleton mineralization (density). Skeletons have an essential function in structure, movement and protection of vertebrates. Although vertebrate skeletons share the same major extracellular components and biological apatite, the skeleton of a group of fishes, the elasmobranchs, differs because it is largely made of a core of unmineralized cartilage covered by a layer of highly mineralized tiles, called *tesserae* [19–21]. As the density of calcium phosphate (hydroxyapatite, or HA,  $\text{Ca}_5(\text{PO}_4)_3(\text{OH})$ ) in the mineralized cartilage is a good predictor of mechanical properties, strength, stiffness and mass of the elasmobranch skeleton [22–24], it is important to understand if ocean acidification and warming interfere with the mechanisms responsible for accumulating and storing phosphate.

In this study, I tested the hypothesis that ocean acidification and warming would affect mineralization of fish skeleton. As far as is known, this is the first study to quantify the effect of these climate change stressors on mineralization in a phosphate system (vertebrates) rather than a carbonate system (invertebrates). In this study, little skate *Leucoraja erinacea* were exposed to simulated current and future ocean conditions throughout embryonic development and continued post-hatching to determine the effect of ocean acidification and warming on juvenile fish. The little skate was chosen as a model organism because considerable work has been conducted using this species, in order to understand the mechanisms underlying the responses of fishes, and in particular elasmobranchs, to climate change stressors and environmental change.

## 2. Material and methods

### (a) Animals and experimental set-up

Newly laid (less than 1 week-old) little skate *L. erinacea* embryos (total  $n = 40$ ,  $n = 10$  replicates per treatment, four treatments) were acquired from the Marine Biological Laboratory (Woods Hole, MA, USA), transported in a thermally stable tank and randomly assigned to a treatment group (one embryo per tank, 10 independent tanks per treatment, a total of 40 independent tanks). Skate embryos were maintained at constant conditions for the duration of their entire development (about five to six months) and after hatching (about two weeks post-hatching). Temperature and  $\text{CO}_2$  levels were chosen to simulate present and future warming and ocean acidification scenarios; 15 and 20°C, 400 and 1100  $\mu\text{atm}$  [2]. Skate embryos were acclimatized to simulated ocean conditions by increasing temperature 0.5°C and 0.05 pH unit, daily until experimental conditions were achieved [25,26].

Embryos and hatchlings were housed in a closed system located inside a temperature-controlled environmental chamber set at 12°C as described previously [12,27]. Briefly, each tank (150 l) was supplied with artificial seawater (Instant Ocean

mixed with deionized water) and independently filtered. The use of Instant Ocean has limitations, as it may cause higher than average alkalinities [28,29]; however, variation in alkalinities was similar to previous studies on the effect of ocean acidification on skates and invertebrates [12,30]. Constant temperature ( $15 \pm 0.05$  or  $20 \pm 0.05^\circ\text{C}$ ) was maintained in each tank by a submersible Finnex 300 W titanium heater controlled by a digital Aqua Logic thermostat. Appropriate levels of  $\text{CO}_2$  (which yield pH values of  $8.07 \pm 0.07$  for treatment 1,  $8.05 \pm 0.08$  for treatment 2 or  $7.70 \pm 0.05$  for treatment 3 and  $7.70 \pm 0.06$  for treatment 4; electronic supplementary material, table 1) were chosen to simulate conditions experienced currently and by the year 2100 according to the climatic model RCP 8.5 [2,31] and by accounting for the predictions that see the Gulf of Maine-Georges Bank area in the northwest Atlantic warming at a faster rate when compared with the global trends [32–34]. To maintain these  $\text{CO}_2$  levels, each tank was independently controlled by an Aqua Medic pH computer (i.e. one pH computer per tank) that triggered the supply of a mixture of air :  $\text{CO}_2$  (water pH 7.7 which resulted in  $\text{pCO}_2$  approx. 1100  $\mu\text{atm}$ ) or was fitted with a line that supplied ambient air (water pH 8.1 which resulted in  $\text{pCO}_2$  approx. 400  $\mu\text{atm}$ ). Total alkalinity was estimated using titration and reference material provided by Andrew Dickson (Scripps Institute of Oceanography). Water parameters were calculated in CO2SYS [35] using suggested constants [36] (electronic supplementary material, table 1). The 40 experiments were not carried out simultaneously but rather in sets, with varying mixed artificial seawater, and this experimental design contributed to the recorded variability in alkalinity (electronic supplementary material, table 1). Temperature and pH levels were checked twice per day using a Traceable NIST (National Institute of Standards and Technology) calibrated thermometer and a Hach® pH meter (Pocket Pro+ pH Tester). Each pH probe was calibrated weekly using buffers. Water quality analyses (ammonia, nitrites, nitrates, salinity and dissolved oxygen) were performed and 30% water changes were made weekly to ensure excellent water quality (no ammonia and nitrites) and constant salinity (33 ppt). Conditions were maintained during water changes by transferring water that was already pre-heated (to either 15 or 20°C from 12°C) and/or after the mixture of air :  $\text{CO}_2$  was already introduced (treatment with pH 7.7). Skates were reared on a 14 L : 10 D photoperiod and, once hatched, were fed daily a diet of frozen mysis shrimp ad libitum.

### (b) Computed tomography scanning procedures and analyses

Natural mortality is relatively high in juvenile skates [27] and those individuals that died around two weeks of age during exposure to treatments in the laboratory were massed, measured and successively skeletal parts closely linked to locomotion (wing or pectoral fin, crus, denticle and vertebra) and feeding (jaw) were dissected out to be analysed (figure 1). All samples were stored in Ringer's solution and frozen until scanning. Skates as well as skeletal parts were photographed and successively digitally measured using IMAGE J [37]. Three-dimensional skeletal density was quantified using micro-computed tomography (micro-CT) imaging (figure 1). Skeletal elements were grouped by type across treatments, mounted in extruded polystyrene rigid foam to eliminate shifts during procedure and scanned with a standard for hydroxyapatite (Scanco Medical) in a plastic container. Skeletal parts were not stained. All parts were scanned at 200  $\mu\text{A}$  and 40 kV for 900 ms with a rotation angle of 0.45° and full 360° rotation (Sky-Scan1173, Micro Photonics, Inc., Allentown, PA, USA). No filter was applied to the camera, and the images were saved as tiff files and produced a voxel size of 25  $\mu\text{m}$ . Slices were reconstructed in NRECON (Micro Photonics, Inc.) and then exported into MIMICS (Materialise, Leuven, Belgium) for analysis of density. Density

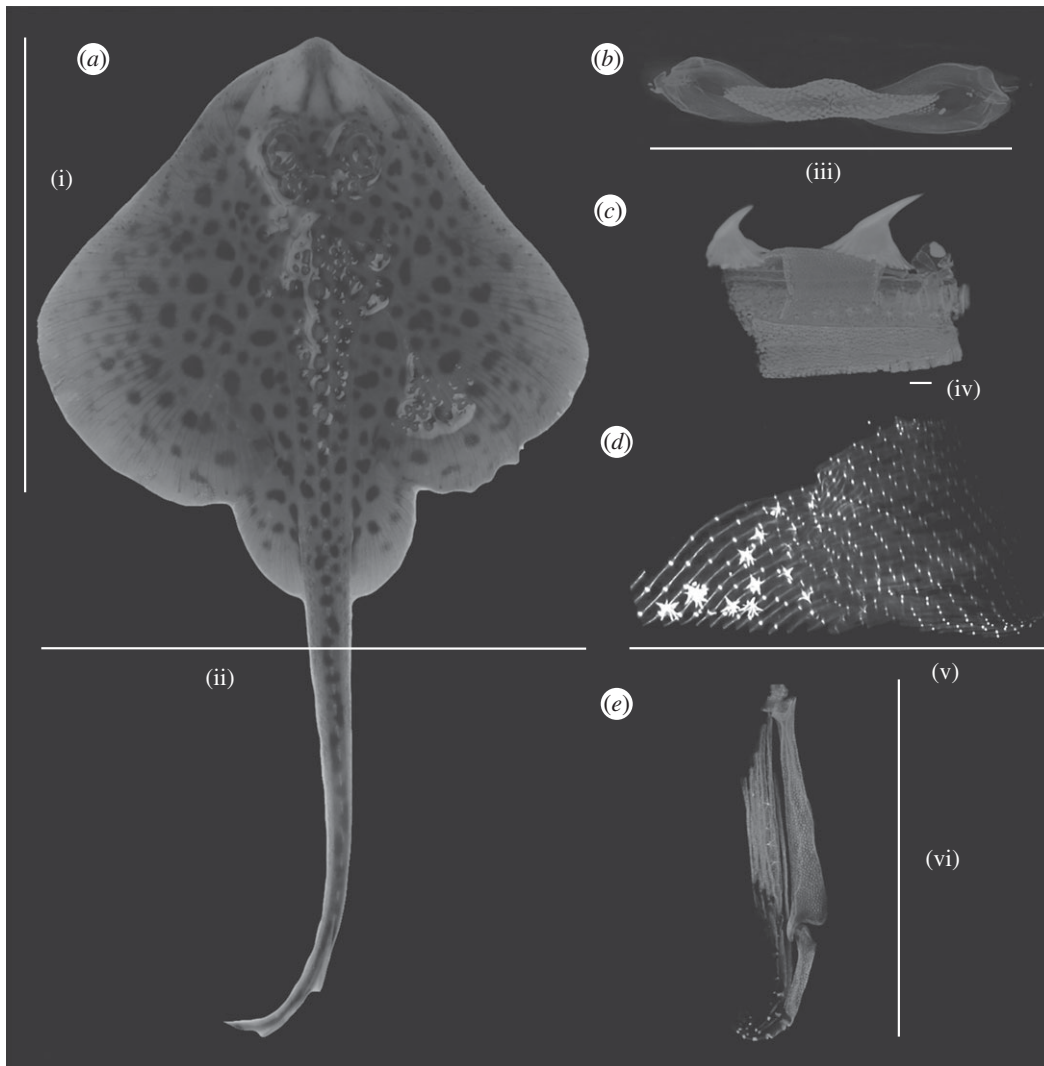


**Figure 1.** Little skate *L. erinacea* (a) skeleton was sampled (b, jaw; c, vertebra; d, wing with denticles; e, crus) to determine cartilage mineralization (as hydroxyapatite density) using micro-CT imaging. From each scan, a three-dimensional model was used to measure and compare mineralization across different treatments. Measurements of skates and each part sampled are indicated (i, disc length; ii, disc width; iii, jaw width; iv, vertebra length; v, wing width; vi, crus length).

data in MIMICS were collected as grey values. Absolute density values ( $\text{mgHA cm}^{-3}$ ) were calculated from grey values using a standard curve derived from the measurements of five hydroxyapatite rods of known density (HA standard) scanned with each sample.

Values of HA density of the tessarated cartilage were averaged from 10 measurements for each part for 10 skates per treatment prior to analyses. The assumptions for normality [38,39] and homogeneity of variance [40] were met ( $p > 0.05$ ), and a two-way analysis of variance (ANOVA) was used to analyse the single and combined effect of  $\text{pCO}_2$  and temperature on HA density. Although, a standard for fluorapatite ( $\text{Ca}_5(\text{PO}_4)_3\text{F}$ ) was not available in this study, grey values (as Hounsfield units) were collected on a subsample of teeth ( $n = 10$  teeth per skate, four skates per treatment) to explore a potential effect of ocean acidification and warming using a two-way ANOVA. The effect of  $\text{pCO}_2$  and temperature was also tested on measurements (cm) of the skeletal parts analysed (wing, crus, vertebra and jaws) as well as on mass, body condition, disc length and width (figure 1). Mean values of different treatments were compared with a control ( $15^\circ\text{C}$ ,  $400 \mu\text{atm}$ ) using a Dunnett's test. If an interaction between factors was found, it was reported following the ANOVA. All analyses were conducted with  $\alpha = 0.05$ . Data were analysed using JMP Pro v. 13 (SAS Institute, Inc.).

### 3. Results

Little skate disc width and body condition were affected by the treatments (two-way ANOVA,  $F_{3,36} = 7.16$ ,  $p < 0.001$

and  $F_{3,36} = 5.50$ ,  $p = 0.003$ , respectively). In particular, while disc width increased with temperature ( $p = 0.002$ , with a significant interaction with  $\text{pCO}_2$ :  $p = 0.006$ , which resulted in a significant difference between treatments and control only at high temperature and  $\text{pCO}_2$ ; Dunnett's test; figure 2), body mass was not significantly affected by temperature ( $p = 0.2$ ) or  $\text{pCO}_2$  ( $p = 0.1$ ). This resulted in a significant reduction of body condition with acidification and temperature ( $p = 0.02$  and  $0.002$ , respectively). Mean body condition was only significantly different at high temperature and  $\text{pCO}_2$  when compared to control conditions (Dunnett's test; figure 2). Disc length was not affected by either temperature or  $\text{pCO}_2$  (two-way ANOVA,  $F_{3,36} = 1.38$ ,  $p = 0.2$ ). Simulated ocean acidification and warming did not affect the length of vertebra (two-way ANOVA,  $F_{3,36} = 1.27$ ,  $p = 0.3$ ). The length of the crus was only significantly reduced as a consequence of  $\text{pCO}_2$  (two-way ANOVA,  $F_{3,36} = 1.27$ ,  $p = 0.03$ ), with no effect of temperature ( $p = 0.09$ ). The Dunnett's test showed that only the mean value of crus length at high temperature and  $\text{pCO}_2$  was statistically different from that of control conditions (figure 2).

Similarly, jaw width significantly declined with  $\text{pCO}_2$  (two-way ANOVA,  $F_{3,36} = 3.15$ ,  $p = 0.005$ ), but temperature had no significant effect ( $p = 0.9$ ). Warming increased significantly the wing width of skates (two-way ANOVA,  $F_{3,36} = 6.10$ ,

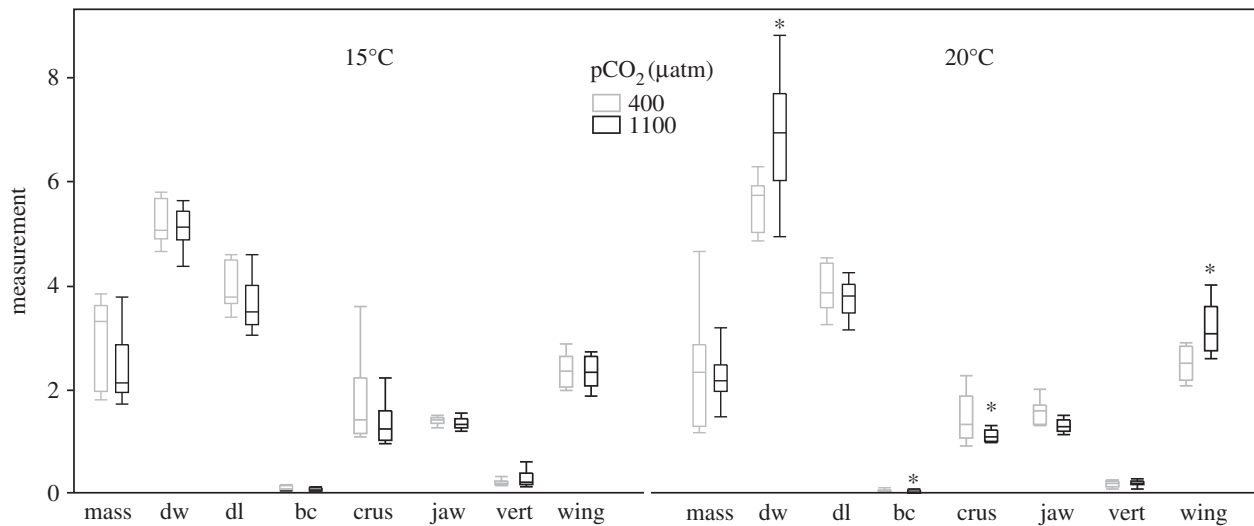


**Figure 2.** Measurements per each part of little skates (mass (g); dw, disc width (cm); dl, disc length (cm); bc, body condition ( $\text{g cm}^{-2}$ ); crus (cm); jaw (cm); vert, vertebra (cm); wing (cm)) developed at four different conditions of temperatures and  $\text{pCO}_2$  (15, 20°C, 400 and 1100  $\mu\text{atm}$ ). Asterisks indicate statistically significant differences in means between treatments and control (15°C and 400  $\mu\text{atm}$ ) using a two-way ANOVA ( $n = 10$ ; factors: temperature and  $\text{CO}_2$ ) followed by Dunnett's test ( $\alpha = 0.05$ ).

$p = 0.007$ ). Although  $\text{pCO}_2$  did not affect wing width ( $p = 0.1$ ), there was a significant interaction between temperature and  $\text{pCO}_2$  ( $p = 0.009$ ). In fact, the Dunnett's test showed that only the mean value at high temperature and  $\text{pCO}_2$  was statistically different from control conditions (figure 2).

Hydroxyapatite density increased significantly with ocean acidification, while it decreased with temperature in some skeletal parts (figure 3). Simulated ocean acidification and warming significantly affected cartilage mineralization of the crus (two-way ANOVA,  $F_{3,36} = 13.64$ ,  $p < 0.001$ ), jaw (two-way ANOVA,  $F_{3,36} = 6.31$ ,  $p = 0.001$ ) and wing (two-way ANOVA,  $F_{3,36} = 7.92$ ,  $p < 0.001$ ). No significant effect of either ocean acidification or warming was detected on the denticle (two-way ANOVA,  $F_{3,36} = 0.81$ ,  $p = 0.5$ ) and the vertebra (two-way ANOVA,  $F_{3,36} = 0.25$ ,  $p = 0.8$ ). The density of HA of the crus significantly increased with acidification ( $p < 0.001$ ) at both temperatures (Dunnett's test; figure 3), while temperature alone did not exert a significant effect ( $p = 0.2$ ). Similarly, HA density increased with acidification in the jaw ( $p = 0.01$ ), with no significant effect of temperature ( $p = 0.06$ ), but there was a significant interacting effect of temperature and  $\text{pCO}_2$  that reduced mineralization at the highest temperature ( $p = 0.006$ ). As a consequence, mean HA was significantly elevated only at 15°C and 1100  $\mu\text{atm}$  when compared with the control (Dunnett's test; figure 3). Wing mineralization significantly decreased with temperature ( $p < 0.001$ ) at both  $\text{pCO}_2$  conditions, with no effect of ocean acidification ( $p = 0.055$ ; Dunnett's test; figure 3). Comparison of grey values on a subset of teeth showed that mineralization was not affected by either temperature ( $p = 0.1$ ) or acidification ( $p = 0.08$ ).

## 4. Discussion

### (a) Ocean acidification and warming alter skeletal mineralization

As far as I know, this is the first study to quantify the effect of ocean acidification and warming on skeleton mineralization of a fish. Overall, simulated ocean acidification *increased* the density of hydroxyapatite in major components of the

skeleton. This result stands in sharp contrast with most previous studies in which the calcium carbonate exoskeleton of marine invertebrates showed a *decrease* in mineralization with ocean acidification [7–9]. Even though some invertebrate species are able to maintain an elevated pH at their site of calcification to maintain constant rates, this comes at a cost [10,11]. In a review of more than 40 studies on the effect of ocean acidification on molluscs, the emerging pattern is that shell calcification is reduced at low pH levels [41]. When the shell or skeleton of calcifying invertebrates is thinner and therefore is more susceptible to fracture, predation pressure increases for these animals [41]. While in marine invertebrates the reduction in  $\text{CaCO}_3$  as a consequence of low pH is owing to a relatively straightforward chemical reaction (i.e.  $\text{H}^+$  precipitates  $\text{Ca}^{2+}$  in the skeleton), the possible mechanism underlying the increase in HA in the skeleton of vertebrates needs further clarification. Here, I outline a few plausible mechanisms that could be responsible for the increase in mineralization in the skeleton of elasmobranch fishes.

First,  $\text{CO}_2$  is a poison, known to affect the neurotransmitter responsible for regulation of  $\text{Ca}^{2+}$  deposition [16,42]. For example, otolith growth and calcification has been shown to be regulated neurally [43]. A study of neuronal control of the calcium supply in the inner ear of cichlid fishes showed a significant precipitation of calcium accumulated at the macular tight junctions [44,45]. It is, in fact, hypothesized that neuronal activity is responsible for the release of calcium into the endolymph of the otolith by altering the permeability of these junctions [43]. Moreover, several studies have now shown that otolith growth and calcification increases, presumably as a result of interference with neural activity, in at least a few larval fishes exposed to elevated  $\text{pCO}_2$  [17,42]. Although cartilage tissue is not deeply innervated, there is evidence that nerve fibres are in contact with the outer layer of cartilage in vertebrates [46]. Neuronal activity, therefore, may regulate not only calcium deposition in the otolith of fishes but also cartilage matrix mineralization and growth.

Another likely mechanism responsible for increased mineralization of cartilage with ocean acidification may be linked to the physiological response of fishes when challenged with

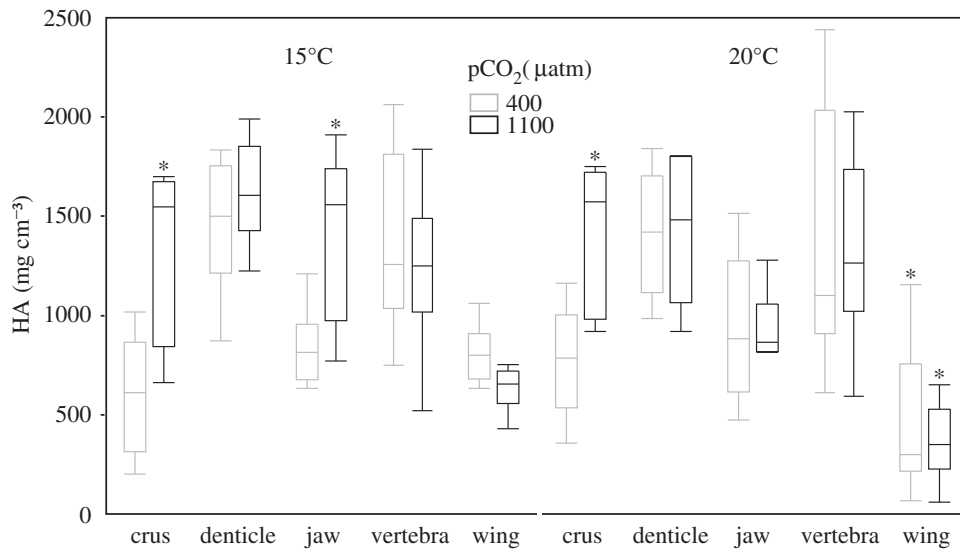


**Figure 3.** HA density ( $\text{mg cm}^{-3}$ ) for each skeletal part sampled at two temperatures (15 and  $20^\circ\text{C}$ ) and  $\text{CO}_2$  conditions (400 and  $1100 \mu\text{atm}$ ). Asterisks indicate statistically significant differences in means between treatments and control ( $15^\circ\text{C}$  and  $400 \mu\text{atm}$ ) using a two-way ANOVA ( $n = 10$ ; factors: temperature and  $\text{CO}_2$ ) followed by Dunnett's test ( $\alpha = 0.05$ ).

fluid acidosis. Fishes are able to compensate for changes in acid–base status within their extracellular body fluids via bicarbonate and non-bicarbonate buffers [47]. In fact, fish gills respond fairly rapidly to acidification by increasing phosphate in body fluids [47–49]. In skates, the increase in buffer capacity is proportional to pH decrease in the water, and skates can achieve acidity compensation within 24 h [50]. Perhaps, this exceptional buffering capacity may have the side effect of accumulating phosphate in blood and tissues and, consequently, in the cartilage. Therefore,  $\text{CO}_2$ -induced acidosis may indirectly contribute to increased skeletal HA density, by increasing phosphate concentration in fish blood. Higher HA density in simulated acidified oceans is, at first, an unexpected result when compared with results from studies on calcifying invertebrates, but a plausible consequence of the effective buffering capacity of elasmobranchs challenged by acidification. In fact, external structures such as denticles and teeth are not affected by acidification. A similar result on denticles was also demonstrated in a previous study on benthic sharks [51], supporting the hypothesis that acidification plays a significant role in physiological processes related to mineralization, rather than a direct effect on the physical structure of the skeleton *per se*, as instead seen in shell-forming invertebrates [41].

Interestingly, warming had an opposite effect on skeleton mineralization. At higher temperature, HA density decreased in the skates' skeleton structures that relate to locomotion, i.e. the wings. The regulation of cartilage mineralization in fishes requires a more in-depth analysis to fully understand the underpinning mechanisms involved in the response to warming. However, previous studies on the effect of climate-related stressors showed that skates challenged by warming had reduced aerobic scope and increased stress [12,52]. Therefore, a reduced mineralization of the skeleton may be an indirect effect of temperature, which reduced the aerobic scope [12,27] and therefore the energy available for physiological processes, such as perhaps skeletal mineralization. It is indeed interesting that the only measured significant differences in mineralization linked to temperature are, in fact, seen in wings which are the skeletal element most closely associated with growth of the animal. In fact, while both disc and wing width increased at the high

temperature and  $\text{pCO}_2$  tested, mass was not significantly affected, thus resulting in a reduction of body condition in conjunction with the reduction in mineralization found in the wing. However, an increase in mineralization was observed in the crura and the jaws regardless of size, suggesting that an increase in mineralization is not necessarily correlated with a slower growth. In this study, no obvious malformations of the skeleton, such as scoliosis, kyphosis or neoplasia, were detected, which were instead reported in several previous studies on larval bony fishes [53–55]. Lastly, there seem to be *no obvious* functional trade-offs of ocean acidification and warming on skeletal mineralization. In other words, the measured changes in skeletal density appear to be side effects of possible neurological, physiological and ecological stressors on fishes which need to maintain homeostasis during acid–base and thermal challenges.

### (b) Ecological consequences of changes in skeletal density and morphology

Changes in skeletal mineralization have the potential to significantly alter performance and energetics of fishes. In fact, the density of HA in the skeleton directly affects mechanical properties and physiological performance [56,57]. Skates may even gain a mechanical advantage at high  $\text{CO}_2$  during feeding by increasing jaw mineralization by 67%. However, when both temperature and  $\text{CO}_2$  were considered, jaw mineralization did not increase significantly. There is a well-established correlation between skeletal mineralization and resistance to deformation from loads [22,23]. Higher mineral content in the cartilage leads to increased stiffness and strength of the skeleton, and, in fact, fishes that reach high speeds during locomotion generally possess a stiffer and stronger skeleton that allows them to transfer energy more effectively. However, wing mineralization was lower at the higher temperature tested (figure 3). Previous work on skates suggests that a large portion of costs of locomotion during swimming at high speeds (approx.  $2 \text{ body lengths s}^{-1}$ ) is derived by the necessity to stiffen the wing through creation of a transversal arch (or a notch) on its margin [16,17]. As a consequence, we would expect that metabolic costs of locomotion might increase even further with fins that are less stiff and need active deformation [58–61].

On the other hand, at low speeds, skates prefer to walk on the substratum using modified fins, the crura [62,63]. Macesic & Summers [64] found that the stiffness of the cartilage in the crura was a good predictor of the ability of batoids to walk. In fact, skates with denser crura were also most likely to exhibit this behaviour [64,65]. In the present study, HA density in the crura was higher under simulated ocean acidification at both temperatures; therefore, skates may increase the frequency of walking under low pH scenarios. The advantages acquired during walking, however, need to be weighed with the consequences of a denser, and hence heavier, skeleton. As the tessellated cartilage becomes more mineralized, buoyancy decreases, thereby reducing locomotor efficiency [66]. Ecological studies have reported that batoid fishes with denser skeletons tend to remain on the bottom of the ocean and are much less active than those with a lower cartilage mineral content [64,65,67]. The sluggish behaviour of benthic elasmobranchs may then be a consequence of the high metabolic costs of swimming incurred with a less buoyant and denser skeleton. Elasmobranchs, in fact, lack a gas bladder, and they need to actively push water downwards to create hydrodynamic lift [68–71]. Interestingly, an increase in metabolic costs during escape responses has already been reported for elasmobranchs under ocean acidification [12], and the present study provides an additional mechanism to explain increased costs of locomotion under simulated future ocean conditions.

Benthic fish species are expected to move to deeper waters to find thermal refugia [72,73]. These deeper cooler waters are characterized by generally higher CO<sub>2</sub> concentrations [9,74,75] and may therefore exacerbate the effect of climate change (through lower pH) on skeleton mineralization. The most intriguing aspect of the results from this study is that ocean acidification and warming have unanticipated consequences on morphology and, consequently,

ecology of marine fishes. We now know that ocean acidification and warming are not only affecting the skeleton of carbonate systems, such as shell-producing invertebrates, but also of phosphate systems, and in particular fishes. Collectively, ecophysiological and morphological studies on the effect of climate change on fishes have demonstrated that many marine species are unlikely to fare well in the near future, especially when they need to cope with a combination of stressors such as warming, acidification, hypoxia, pollution, habitat destruction, and overfishing, which can all reduce physiological performance and resilience under future scenarios.

**Ethics.** Skates were maintained under the approved Institutional Animal Care and Use protocol no. 11-041 at Boston University, and the micro-CT scans on naturally deceased skates were performed at the Museum of Comparative Zoology, Harvard University.

**Data accessibility.** The dataset supporting this article has been uploaded as part of the electronic supplementary material. Skate samples used in this project have been deposited in the Museum of Comparative Zoology at Harvard University (MCZ catalogue no. 173199, 173200, 173201 and 173202).

**Authors' contributions.** V.D.S. conceived, planned, executed the experiments, analysed the data, made the figures and wrote the manuscript.

**Competing interests.** The author declares no conflict of interest.

**Funding.** This research was supported by the Steven Berkeley Marine Conservation Fellowship (to V.D.S.), the Museum of Comparative Zoology at Harvard University and the Office of Naval Research Multi-University Research Initiative Grant N000141410533 monitored by Dr Bob Brizzolara (to George Lauder).

**Acknowledgements.** I thank George Lauder for critical logistic and conceptual support, Dylan Wainwright and Andy Williston for guidance during acquisition of the CT scans, and Elise Morgan for providing the hydroxyapatite standards used in this study. Two anonymous reviewers provided insightful comments on a previous version of this manuscript. I thank Mason Dean for interesting conversations on elasmobranch cartilage.

## References

- Raven J, Caldeira K, Elderfield H, Hoegh-Guldberg O, Liss P, Riebesell U, Shepherd J, Turley C, Watson A. 2005 *Ocean acidification due to increasing atmospheric carbon dioxide*. London, UK: The Royal Society.
- Intergovernmental Panel on Climate Change. 2015 *Climate change 2014: mitigation of climate change*. New York, NY: Cambridge University Press.
- Somero G. 2010 The physiology of climate change: how potentials for acclimatization and genetic adaptation will determine 'winners' and 'losers'. *J. Exp. Biol.* **213**, 912–920. (doi:10.1242/jeb.037473)
- Fry FJ. 1967 Responses of vertebrate poikilotherms to temperature. *Thermobiol. Acad. Press N. Y.* 375–409.
- Di Santo V, Bennett WA. 2011 Is post-feeding thermotaxis advantageous in elasmobranch fishes? *J. Fish Biol.* **78**, 195–207. (doi:10.1111/j.1095-8649.2010.02853.x)
- Angilletta MJ. 2009 *Thermal adaptation: a theoretical and empirical synthesis*. Oxford, UK: Oxford University Press.
- Bednaršek N, Tarling GA, Bakker DC, Fielding S, Feely RA. 2014 Dissolution dominating calcification process in polar pteropods close to the point of aragonite undersaturation. *PLoS ONE* **9**, e109183. (doi:10.1371/journal.pone.0109183)
- Chatziniakolaou E, Grigoriou P, Keklikoglou K, Faulwetter S, Papageorgiou N. 2016 The combined effects of reduced pH and elevated temperature on the shell density of two gastropod species measured using micro-CT imaging. *ICES J. Mar. Sci.* **74**, 1135–1149.
- Feely RA, Sabine CL, Lee K, Berelson W, Kleypas J, Fabry VJ, Millero FJ. 2004 Impact of anthropogenic CO<sub>2</sub> on the CaCO<sub>3</sub> system in the oceans. *Science* **305**, 362–366. (doi:10.1126/science.1097329)
- Ries JB, Cohen AL, McCorkle DC. 2009 Marine calcifiers exhibit mixed responses to CO<sub>2</sub>-induced ocean acidification. *Geology* **37**, 1131–1134. (doi:10.1130/G30210A.1)
- Seibel BA, Maas AE, Dierssen HM. 2012 Energetic plasticity underlies a variable response to ocean acidification in the pteropod, *Limacina helicina antarctica*. *PLoS ONE* **7**, e30464. (doi:10.1371/journal.pone.0030464)
- Di Santo V. 2016 Intraspecific variation in physiological performance of a benthic elasmobranch challenged by ocean acidification and warming. *J. Exp. Biol.* **219**, 1725–1733. (doi:10.1242/jeb.139204)
- Ishimatsu A, Hayashi M, Kikkawa T. 2008 Fishes in high-CO<sub>2</sub>, acidified oceans. *Mar. Ecol. Prog. Ser.* **373**, 295–302. (doi:10.3354/meps07823)
- Munday PL, Dixon DL, Donelson JM, Jones GP, Pratchett MS, Devitsina GV, Døving KB. 2009 Ocean acidification impairs olfactory discrimination and homing ability of a marine fish. *Proc. Natl Acad. Sci. USA* **106**, 1848–1852. (doi:10.1073/pnas.0809996106)
- Simpson SD, Munday PL, Wittenrich ML, Manassa R, Dixon DL, Gagliano M, Yan HY. 2011 Ocean acidification erodes crucial auditory behaviour in a marine fish. *Biol. Lett.* **7**, 917. (doi:10.1098/rsbl.2011.0293)
- Bignami S, Enochs IC, Manzello DP, Sponaugle S, Cowen RK. 2013 Ocean acidification alters the otoliths of a pantropical fish species with implications for sensory function. *Proc. Natl Acad. Sci. USA* **110**, 7366–7370. (doi:10.1073/pnas.1301365110)

17. Checkley DM, Dickson AG, Takahashi M, Radich JA, Eisenkolb N, Asch R. 2009 Elevated CO<sub>2</sub> enhances otolith growth in young fish. *Science* **324**, 1683. (doi:10.1126/science.1169806)
18. Munday PL, Hernaman V, Dixon DL, Thorold SR. 2011 Effect of ocean acidification on otolith development in larvae of a tropical marine fish. *Biogeosciences* **8**, 1631–1641. (doi:10.5194/bg-8-1631-2011)
19. Dean MN, Chiou W-A, Summers AP. 2005 Morphology and ultrastructure of prismatic calcified cartilage. *Microsc. Microanal.* **11**, 1196.
20. Dean MN, Mull CG, Gorb SN, Summers AP. 2009 Ontogeny of the tessellated skeleton: insight from the skeletal growth of the round stingray *Urolophus halleri*. *J. Anat.* **215**, 227–239. (doi:10.1111/j.1469-7580.2009.01116.x)
21. Dean MN, Summers AP. 2006 Mineralized cartilage in the skeleton of chondrichthyan fishes. *Zoology* **109**, 164–168. (doi:10.1016/j.zool.2006.03.002)
22. Balaban JP, Summers AP, Wilga CA. 2015 Mechanical properties of the hyomandibula in four shark species. *J. Exp. Zool. Part Ecol. Genet. Physiol.* **323**, 1–9. (doi:10.1002/jez.1888)
23. Porter ME, Koob TJ, Summers AP. 2007 The contribution of mineral to the material properties of vertebral cartilage from the smooth-hound shark *Mustelus californicus*. *J. Exp. Biol.* **210**, 3319–3327. (doi:10.1242/jeb.006189)
24. Wilga CAD, Diniz SE, Steele PR, Sudario-Cook J, Dumont ER, Ferry LA. 2016 Ontogeny of feeding mechanics in smoothhound sharks: morphology and cartilage stiffness. *Integr. Comp. Biol.* **56**, 442–448. (doi:10.1093/icb/icw078)
25. Fangué NA, Bennett WA. 2003 Thermal tolerance responses of laboratory-acclimated and seasonally acclimated Atlantic stingray, *Dasyatis sabina*. *Copeia* **2003**, 315–325. (doi:10.1643/0045-8511(2003)003[0315:TTROLA]2.0.CO;2)
26. Di Santo V, Jordan HL, Cooper B, Currie RJ, Beitinger TL, Bennett WA. 2018 Thermal tolerance of the invasive red-bellied pacu and the risk of establishment in the United States. *J. Therm. Biol.* **74**, 110–115. (doi:10.1016/j.jtherbio.2018.03.015)
27. Di Santo V. 2015 Ocean acidification exacerbates the impacts of global warming on embryonic little skate, *Leucoraja erinacea* (Mitchill). *J. Exp. Mar. Biol. Ecol.* **463**, 72–78. (doi:10.1016/j.jembe.2014.11.006)
28. Ingersoll CG, Dwyer F, Burch S, Nelson M, Buckler D, Hunn J. 1992 The use of freshwater and saltwater animals to distinguish between the toxic effects of salinity and contaminants in irrigation drain water. *Environ. Toxicol. Chem. Int. J.* **11**, 503–511. (doi:10.1002/etc.5620110408)
29. Havach SM, Chandler GT, Wilson-Finelli A, Shaw TJ. 2001 Experimental determination of trace element partition coefficients in cultured benthic foraminifera. *Geochim. Cosmochim. Acta* **65**, 1277–1283. (doi:10.1016/S0016-7037(00)00563-9)
30. McDonald MR, McClintock JB, Amsler CD, Rittschof D, Angus RA, Orihuela B, Lutostanski K. 2009 Effects of ocean acidification over the life history of the barnacle *Amphibalanus amphitrite*. *Mar. Ecol. Prog. Ser.* **385**, 179–187. (doi:10.3354/meps08099)
31. Riebesell U, Fabry VJ, Hansson L, Gattuso J-P. 2011 *Guide to best practices for ocean acidification research and data reporting*. Luxembourg: Office for Official Publications of the European Communities.
32. Pershing AJ *et al.* 2015 Slow adaptation in the face of rapid warming leads to collapse of the Gulf of Maine cod fishery. *Science* **350**, 809–812. (doi:10.1126/science.aac9819)
33. Belkin IM. 2009 Rapid warming of large marine ecosystems. *Prog. Oceanogr.* **81**, 207–213. (doi:10.1016/j.pocean.2009.04.011)
34. Saba VS *et al.* 2016 Enhanced warming of the Northwest Atlantic Ocean under climate change. *J. Geophys. Res. Oceans* **121**, 118–132. (doi:10.1002/2015JC011346)
35. Pierrot D, Lewis E, Wallace D. 2006 *MS Excel program developed for CO<sub>2</sub> system calculations*. ORNLCDIAC-105a. Oak Ridge, TN: Carbon Dioxide Inf. Anal. Cent. Oak Ridge Natl. Lab. U.S. Dep. Energy Oak Ridge Tenn.
36. Dickson A, Millero F. 1987 A comparison of the equilibrium constants for the dissociation of carbonic acid in seawater media. *Deep Sea Res. Part Oceanogr. Res. Pap.* **34**, 1733–1743. (doi:10.1016/0198-0149(87)90021-5)
37. Schneider CA, Rasband WS, Eliceiri KW. 2012 NIH Image to ImageJ: 25 years of image analysis. *Nat. Methods* **9**, 671. (doi:10.1038/nmeth.2089)
38. Anderson TW, Darling DA. 1954 A test of goodness of fit. *J. Am. Stat. Assoc.* **49**, 765–769. (doi:10.1080/01621459.1954.10501232)
39. D'Agostino R, Pearson ES. 1973 Tests for departure from normality. Empirical results for the distributions of  $b^2$  and  $\sqrt{b^1}$ . *Biometrika* **60**, 613–622.
40. Brown MB, Forsythe AB. 1974 Robust tests for the equality of variances. *J. Am. Stat. Assoc.* **69**, 364–367. (doi:10.1080/01621459.1974.10482955)
41. Gazeau F, Parker LM, Comeau S, Gattuso J-P, O'Connor WA, Martin S, Pörtner H-O, Ross PM. 2013 Impacts of ocean acidification on marine shelled molluscs. *Mar. Biol.* **160**, 2207–2245. (doi:10.1007/s00227-013-2219-3)
42. Bignami S, Sponaugle S, Cowen RK. 2013 Response to ocean acidification in larvae of a large tropical marine fish, *Rachycentron canadum*. *Glob. Change Biol.* **19**, 996–1006. (doi:10.1111/gcb.12133)
43. Anken RH. 2006 On the role of the central nervous system in regulating the mineralisation of inner-ear otoliths of fish. *Protoplasma* **229**, 205–208. (doi:10.1007/s00709-006-0219-6)
44. Beier M, Anken R, Rahmann H. 2004 Calcium-tracers disclose the site of biomineralization in inner ear otoliths of fish. *Adv. Space Res.* **33**, 1401–1405. (doi:10.1016/j.asr.2003.09.044)
45. Ibsch M, Anken R, Beier M, Rahmann H. 2004 Endolymphatic calcium supply for fish otolith growth takes place via the proximal portion of the otocyst. *Cell Tissue Res.* **317**, 333–336. (doi:10.1007/s00441-004-0930-6)
46. Grässel S. 2014 The role of peripheral nerve fibers and their neurotransmitters in cartilage and bone physiology and pathophysiology. *Arthritis Res. Ther.* **16**, 485. (doi:10.1186/s13075-014-0485-1)
47. Evans DH, Piermarini PM, Choe KP. 2005 The multifunctional fish gill: dominant site of gas exchange, osmoregulation, acid-base regulation, and excretion of nitrogenous waste. *Physiol. Rev.* **85**, 97–177. (doi:10.1152/physrev.00050.2003)
48. Gilmour KM, Shah B, Szebedinszky C. 2002 An investigation of carbonic anhydrase activity in the gills and blood plasma of brown bullhead (*Ameiurus nebulosus*), longnose skate (*Raja rhina*), and spotted ratfish (*Hydrolagus colliie*). *J. Comp. Physiol. B* **172**, 77–86. (doi:10.1007/s003600100229)
49. Wright PA, Wood CM. 2015 Regulation of ions, acid–base, and nitrogenous wastes in elasmobranchs. In *Fish physiology* (eds RE Shadwick, AP Farrell, CJ Brauner), pp. 279–345. Cambridge, MA: Academic Press.
50. Graham MS, Turner JD, Wood CM. 1990 Control of ventilation in the hypercapnic skate *Raja ocellata*. I. Blood and extracellular fluid. *Respir. Physiol.* **80**, 259–277. (doi:10.1016/0034-5687(90)90088-G)
51. Green L, Jutfelt F. 2014 Elevated carbon dioxide alters the plasma composition and behaviour of a shark. *Biol. Lett.* **10**, 20140538. (doi:10.1098/rsbl.2014.0538)
52. Di Santo V, Tran AH, Svendsen JC. 2016 Progressive hypoxia decouples activity and aerobic performance of skate embryos. *Conserv. Physiol.* **4**, cov067. (doi:10.1093/conphys/cov067)
53. Chambers R, Candelmo A, Habeck E, Poach M, Wiczorek D, Cooper K, Greenfield C, Phelan B. 2014 Effects of elevated CO<sub>2</sub> in the early life stages of summer flounder, *Paralichthys dentatus*, and potential consequences of ocean acidification. *Biogeosciences* **11**, 1613–1626. (doi:10.5194/bg-11-1613-2014)
54. Baumann H, Talmage SC, Gobler CJ. 2012 Reduced early life growth and survival in a fish in direct response to increased carbon dioxide. *Nat. Clim. Change* **2**, 38.
55. Hurst TP, Fernandez ER, Mathis JT, Miller JA, Stinson CM, Ahgeak EF. 2012 Resiliency of juvenile walleye pollock to projected levels of ocean acidification. *Aquat. Biol.* **17**, 247–259. (doi:10.3354/ab00483)
56. Porter ME, Long JH. 2010 Vertebrae in compression: mechanical behavior of arches and centra in the gray smooth-hound shark (*Mustelus californicus*). *J. Morphol.* **271**, 366–375.
57. Serrat MA. 2014 Environmental temperature impact on bone and cartilage growth. *Compr. Physiol.* **4**, 621–655. (doi:10.1002/cphy.c130023)
58. Di Santo V, Blevins EL, Lauder GV. 2017 Batoid locomotion: effects of speed on pectoral fin deformation in the little skate, *Leucoraja erinacea*. *J. Exp. Biol.* **220**, 705–712. (doi:10.1242/jeb.148767)
59. Schaefer JT, Summers AP. 2005 Batoid wing skeletal structure: novel morphologies, mechanical implications, and phylogenetic patterns. *J. Morphol.* **264**, 298–313. (doi:10.1002/jmor.10331)
60. Di Santo V, Kenaley CP. 2016 Skating by: low energetic costs of swimming in a batoid fish. *J. Exp. Biol.* **219**, 1804–1807. (doi:10.1242/jeb.136358)

61. Di Santo V, Kenaley CP, Lauder GV. 2017 High postural costs and anaerobic metabolism during swimming support the hypothesis of a U-shaped metabolism–speed curve in fishes. *Proc. Natl Acad. Sci. USA* **114**, 13 048–13 053. (doi:10.1073/pnas.1715141114)
62. Bilecenoglu M, Ekstrom L. 2013 Pelvic fin walking and punting behaviour of *Raja radula* Delaroche, 1809 observed in the Sea of Marmara. *Mediterr. Mar. Sci.* **14**, 158–161. (doi:10.12681/mms.333)
63. Koester DM, Spirito CP. 2003 Punting: an unusual mode of locomotion in the little skate, *Leucoraja erinacea* (Chondrichthyes: Rajidae). *Copeia* **2003**, 553–561. (doi:10.1643/CG-02-153R1)
64. Macesic LJ, Summers AP. 2012 Flexural stiffness and composition of the batoid propterygium as predictors of punting ability. *J. Exp. Biol.* **215**, 2003–2012. (doi:10.1242/jeb.061598)
65. Bigelow H, Schroeder W. 1953 *Sawfishes, guitarfishes, skates and rays*. New Haven, CT: Sears Foundation for Marine Research.
66. Alexander RM. 1993 Buoyancy. In *The physiology of fishes* (ed. DH Evans), pp. 75–97. Boca Raton, FL: CRC Press.
67. Mollet H. 2002 Distribution of the pelagic stingray, *Dasyatis violacea* (Bonaparte, 1832), off California, Central America, and worldwide. *Mar. Freshw. Res.* **53**, 525–530. (doi:10.1071/MF02010)
68. Lauder GV, Di Santo V. 2015 Swimming mechanics and energetics of elasmobranch fishes. In *Fish physiology* (eds RE Shadwick, AP Farrell, CJ Brauner), pp. 219–253. Cambridge, MA: Academic Press.
69. Wilga CA, Lauder GV. 2004 Biomechanics of locomotion in sharks, rays, and chimeras. In *Biology of sharks and their relatives* (eds JC Carrier, JA Musick, MR Heithaus), pp. 139–164. Boca Raton, FL: CRC Press.
70. Wilga CD, Lauder GV. 2000 Three-dimensional kinematics and wake structure of the pectoral fins during locomotion in leopard sharks *Triakis semifasciata*. *J. Exp. Biol.* **203**, 2261–2278.
71. Park S-J *et al.* 2016 Phototactic guidance of a tissue-engineered soft-robotic ray. *Science* **353**, 158–162. (doi:10.1126/science.aaf4292)
72. Nye JA, Link JS, Hare JA, Overholtz WJ. 2009 Changing spatial distribution of fish stocks in relation to climate and population size on the Northeast United States continental shelf. *Mar. Ecol. Prog. Ser.* **393**, 111–129. (doi:10.3354/meps08220)
73. Perry AL, Low PJ, Ellis JR, Reynolds JD. 2005 Climate change and distribution shifts in marine fishes. *Science* **308**, 1912–1915. (doi:10.1126/science.1111322)
74. Sabine CL *et al.* 2004 The oceanic sink for anthropogenic CO<sub>2</sub>. *Science* **305**, 367–371. (doi:10.1126/science.1097403)
75. Toggweiler J. 1999 Variation of atmospheric CO<sub>2</sub> by ventilation of the ocean's deepest water. *Paleoceanography* **14**, 571–588. (doi:10.1029/1999PA900033)